Contribution from the Department of Natural Sciences, Baruch College, Manhattan, New York 10010, and Department of Chemistry, Brookhaven National Laboratory, Upton, New York 11973

Electron-Transfer Barriers and Metal–Ligand Bonding as a Function of Metal Oxidation State. 2. Crystal and Molecular Structures of Tris(2,2′-bipyridine)cobalt(II) Dichloride–2-Water–Ethanol and Tris(2,2′-bipyridine)cobalt(I) Chloride–Water[1]

DAVID J. SZALDA,[2a,b] CAROL CREUTZ,*[2b] DEVINDER MAHAJAN,[2b] and NORMAN SUTIN[2b]

Received November 11, 1982

The structures of tris(2,2′-bipyridine)cobalt(II) dichloride–2-water–ethanol, $[Co(C_{10}H_8N_2)_3]Cl_2 \cdot 2H_2O \cdot C_2H_5OH$ (**1**), and tris(2,2′-bipyridine)cobalt(I) chloride–water, $Co(C_{10}H_8N_2)_3Cl \cdot H_2O$ (**2**), have been determined in order to compare bonding of the high-spin d^7 and high-spin d^8 configurations and to better understand the electron-transfer reactivity of this couple. Compound **1** crystallizes in the hexagonal crystal system, space group $P6_522$, with a = 13.403 (2) Å, c = 62.566 (10) Å, and Z = 12. The structure refined to a final R value of 0.056. The coordination sphere consists of the six nitrogen atoms of the three bipyridine ligands in an octahedral arrangement about the cobalt with an average Co–N bond length of 2.128 (8) Å. One of the chloride ions is surrounded by twelve C–H···Cl hydrogen bonds involving the H3 and H3′ protons on the bipyridine ligands. Compound **2** crystallizes in the orthorhombic crystal system, space group $Pna2_1$, with a = 9.713 (6) Å, b = 21.666 (10) Å, c = 13.062 (7) Å, and Z = 4. The structure refined to a final R value of 0.084. The geometry of the coordination sphere of **2** is almost identical with that of **1**, with an average Co–N bond length of 2.11 (2) Å. Hydrogen bonding between the H3 and H3′ protons on the bipyridine ligand and the chloride ion is also observed in **2**. The C–H···Cl hydrogen bonding observed in these complexes and the bond length changes in **1**, **2**, and tris(2,2′-bipyridine)cobalt(III) are discussed and related to electron-transfer barriers for the series.

Introduction

The changes in metal–ligand bond lengths that result from oxidation or reduction of a metal complex provide important information on the metal–ligand binding itself and are an important factor in determining the intrinsic reactivity of the couple with respect to oxidation or reduction.[3,4] Thus, the nearly identical Fe(II)–N and Fe(III)–N bond lengths in the 1,10-phenanthroline (phen) complexes $Fe(phen)_3^{2+}$ and $Fe(phen)_3^{3+}$,[3,5,6] in contrast to the 0.13-Å Fe–O bond length difference for $Fe(H_2O)_6^{2+}$ and $Fe(H_2O)_6^{3+}$,[3,7,8] reflect significant Fe(II)-to-phen π-back-bonding in $Fe(phen)_3^{2+}$, which is responsible, in part, for the intrinsically greater reactivity of the $Fe(phen)_3^{2+}$–$Fe(phen)_3^{3+}$ couple toward outer-sphere electron-transfer reactions. Metal–ligand bond length data have been determined for a number of six-coordinate divalent and trivalent complexes of iron, cobalt, and ruthenium with ligands such as water, ammonia, and bpy (2,2′-bipyridine) or phen.[3] By contrast, few data exist for six-coordinate divalent and monovalent couples. Here we report structural data for $Co(bpy)_3^{2+}$ and $Co(bpy)_3^{+}$.

Our interest in the cobalt bipyridine complexes arises for several reasons. First, the structure of $Co(bpy)_3^{+}$ is of considerable current interest because its reaction with water leads to nearly stoichiometric production of H_2 and $Co(bpy)_3^{2+}$.[9] Solids containing $Co(bpy)_3^{+}$ have long been known[10,11] and described as high-spin d^8 cobalt(I), a formulation in accord with the magnetic susceptibility 2.53[11a]–2.89[10b] μ_B recorded for the ClO_4^- salt (for high-spin d^8 $Ni(bpy)_3^{2+}$, μ_{eff} = 2.88 μ_B), the vis–near-IR spectrum (which has been modeled as a series of metal-to-ligand charge-transfer transitions),[11a] and the UV spectrum;[11b] the proton NMR spectrum of $Co(bpy)_3^{+}$ has been taken as evidence for $\sigma d \rightarrow$ bpy π spin delocalization.[11b] Our structural results confirm the description of $Co(bpy)_3^{+}$ as a tris chelated complex containing six metal–nitrogen bonds and suggest significant metal-to-ligand electron donation in this low-oxidation-state species. In addition, our results enable comparison of metal–bpy bonding for the high-spin d^8 cobalt(I) and high-spin d^7 cobalt(II) configurations, electronic configurations that, like low-spin d^6 (e.g., $Fe(phen)_3^{2+}$) and low-spin d^5 (e.g., $Fe(phen)_3^{3+}$), differ in the occupancy of the πd metal orbitals and provide insight into the high outer-sphere electron-transfer reactivity of the $Co(bpy)_3^{+}$–$Co(bpy)_3^{2+}$ couple.[3,9]

Experimental Section

Preparation of $Co(bpy)_3Cl \cdot H_2O$ and $Co(bpy)_3Cl_2 \cdot 2H_2O \cdot C_2H_5OH$. Both cobalt(I)[9,10] and cobalt(II)[12] complexes were prepared by literature methods. The crystals used were grown as follows:

$[Co(bpy)_3]Cl_2$. To a pink solution of $CoCl_2 \cdot 6H_2O$ (0.24 g, 1 mmol) in ethanol (5 mL) was added an ethanol solution of bpy (0.78 g, 5 mmol). The resulting yellow solution was filtered, topped with 20 mL of diethyl ether (without stirring or mixing), and allowed to stand overnight. The orange crystals so obtained were washed a few times with ether and were dried by blowing argon through the Schlenk tube.

$[Co(bpy)_3]Cl$. For recrystallization, the dark solid (~0.2 g) was dissolved in dry ethanol (~2 mL) in a Schlenk tube. Benzene (10 mL) was added, and the solution was stirred. Diethyl ether (20 mL) was added to the blue solution, and the Schlenk tube was kept (without stirring) in the glovebox. After ~3 days, dark blue/black crystals formed. The crystals were washed with ether and dried by blowing argon over the crystals.

Collection and Reduction of X-ray Data

Tris(2,2′-bipyridine)cobalt(II) Dichloride–2-Water–Ethanol (1). This compound crystallizes as orange hexagonal prisms. The crystals decomposed in air, so they were coated with petroleum jelly and enclosed in Lindemann glass capillary tubes. This was done in a glovebag under an argon atmosphere. Precession photographs indicated $6/mmm$ Laue symmetry with a very long c axis. Because of this 62.566-Å axis, copper radiation was used to collect the intensity data. A diffractometer study on a crystal of **1** confirmed the crystal class and revealed the systematic absences $00l$, $l = 6n + 1, \ldots, 5$, consistent with the enantiomorphic pair of space groups $P6_122$ (D_6^2, No. 178)[13a] and $P6_522$ (D_6^3, No. 179).[13b] The space group $P6_122$ was used for the solution and initial refinement of the structure. After all of the non-hydrogen atoms except for one water molecule had been

(1) Part 1 in this series is ref 3.
(2) (a) Baruch College. (b) Brookhaven National Laboratory.
(3) Brunschwig, B. S.; Creutz, C.; Macartney, D. H.; Sham, T. K.; Sutin, N. *Discuss. Faraday Soc.* **1982**, *74*, 113.
(4) Sutin, N. *Acc. Chem. Res.* **1982**, *15*, 275. Sutin, N. *Annu. Rev. Nucl. Sci.* **1962**, *12*, 285 and references cited therein.
(5) Zalkin, A.; Templeton, D. H.; Ueki, T. *Inorg. Chem.* **1973**, *12*, 1641.
(6) Baker, J.; Engelhardt, L. M.; Figgis, B. N.; White, A. H. *J. Chem. Soc., Dalton Trans.* **1975**, 530.
(7) Beattie, J. K.; Best, S. P.; Skelton, B. W.; White, A. H. *J. Chem. Soc., Dalton Trans.* **1981**, 2105.
(8) Carrell, H. L.; Glusker, J. P. *Acta Crystallogr., Sect. B* **1973**, *B29*, 638.
(9) Krishnan, C. V.; Creutz. C.; Mahajan, D.; Schwarz, H. A.; Sutin, N. *Isr. J. Chem.* **1982**, *22*, 98.
(10) (a) Waind, G. M.; Martin, B. *J. Inorg. Nucl. Chem.* **1958**, *8*, 551. (b) Martin, B.; McWhinnie, W. R.; Waind, G. M. *Ibid.* **1961**, *23*, 207.
(11) (a) Kaizu, Y.; Torii, Y.; Kobayashi, H. *Bull. Chem. Soc. Jpn.* **1970**, *43*, 3296. (b) Fitzgerald, R. J.; Hutchinson, B. B.; Nakamoto, K. *Inorg. Chem.* **1970**, *9*, 2618.
(12) Burstall, F. H.; Nyholm, R. S. *J. Chem. Soc.* **1952**, 3570.
(13) "International Tables for X-ray Crystallography", 3rd ed.; Kynoch Press: Birmingham, England, 1969; Vol. I: (a) p 285; (b) p 286; (c) p 119; (d) p 151.

0020-1669/83/1322-2372$01.50/0

Table I. Experimental Details of the X-ray Diffraction Study

	$Co(C_{10}H_8N_2)_3Cl_2\cdot 2H_2O\cdot C_2H_5OH$ (1)	$Co(C_{10}H_8N_2)_3Cl\cdot H_2O$ (2)
	(A) Crystal Parameters	
a, Å	13.403 (2)	9.713 (6)
b, Å		21.666 (10)
c, Å	62.566 (10)	13.062 (7)
V, Å^3	9733.6	2748.8
Z	12	4
mol wt	680.5	581.0
space group	$P6_522$	$Pna2_1$
ρ(exptl), g cm^{-3}	1.38	
ρ(calcd), g cm^{-3}	1.393	1.404
	(B) Measurement of Intensity Data	
instrument	Enraf-Nonius Cad-4 diffractometer	
radiation	Cu Kα (1.540 51 Å) graphite monochromatized	Mo Kα (0.7093 Å) graphite monochromatized
2θ limits, deg	2–124	data set I: 2–40 data set II: 2–46
scan type	θ(crystal)–2θ(counter)	
stds	3 reflections (0,0,12), ($2\bar{3}6$), and ($\bar{2}16$) measured after each 1 h of exposure time; these standards displayed only random variations over the course of data collection	3 reflections ($\bar{1}20$), (062), and (232) measured after each 0.5 h of exposure time; these standards decayed by 46–53% during data set I collection and by 26–37% during data set II collection
	(C) Treatment of Intensity Data	
reduction to F_o and $\sigma(F_o)$	correction for background, attenuators, and Lorentz–polarization effects of monochromatized X radiation in the usual manner[a]	
abs cor[b]	μ = 59.22 cm^{-1}; max and min transmission coefficients 0.2817 and 0.1750, respectively	μ = 7.83 cm^{-1}; no absorption corrections applied because of the small value of μ and the decay of the crystal data during collection
obsd data	5269 observed reflections combined to yield 2923 unique reflections with an R_{av} = 0.026; 2032 reflections having $F_o > 3\sigma(F_o)$ used in the refinement	2031 observed reflections from I (*hkl* and $h\bar{k}l$) and the 1462 observed reflections from II (*hkl*) put on a common scale[c] and combined to yield 1660 unique reflections with an R_{av} = 0.031; 977 reflections having $F_o > 3\sigma(F_o)$ used in the refinement

[a] Data reduction and corrections performed by using the program KAPPA, part of the CRYSNET system at Brookhaven National Laboratory. [b] Absorption correction computed by using ABSOR, part of the CRYSNET system at Brookhaven National Laboratory. [c] The data from the two crystals were put on a common scale[15] by using common reflections and the linear least-squares method of Rae and Blake (*Acta Crystallogr.* **1966**, *20*, 586).

located, the enantiomorphic structure in space group $P6_522$ was observed to give a lower R_2[14] value than $P6_122$, so the space group was switched to $P6_522$.

The crystal used for data collection was a hexagon of dimensions 0.30 mm × 0.33 mm × 0.33 mm × 0.55 mm. Crystal data and details of data collection and reduction are given in Table I. The *hkl* and $\bar{h}\bar{k}l$ reflections where $|h| \leq |k|$ were collected. The 5269 nonzero reflections were averaged to yield 2923 unique reflections with an R_{av} = 0.026.[15]

Tris(2,2′-bipyridine)cobalt(I) Chloride–Water (2). Crystals of **2** decompose quickly when exposed to the air. Various procedures were attempted in order to prevent crystal decomposition. Several crystals, some coated with petroleum jelly and some without, were mounted in Lindemann glass capillary tubes under an argon atmosphere in either a glovebag or a glovebox. In every case the crystals exhibited a rapid decrease in their ability to diffract X-rays. After storage in a glovebox under an argon atmosphere for about 2 months, all the crystals in the sample had decomposed. The crystal density was not measured. Several different crystals were studied on the diffractometer and showed *mmm* Laue symmetry with systematic absences $0kl$, $k + l = 2n + 1$, and $h0l$, $h = 2n + 1$, consistent with the space groups $Pna2_1$ (C_{2v}^9, No. 33)[13c] and *Pnam* (a nonstandard setting of *Pnma* (D_{2h}^{16}, No. 62)).[13d] *E* statistics indicated a noncentrosymmetric structure, and therefore the acentric space group $Pna2_1$ was chosen for the subsequent refinement of the structure. (Attempts to refine the structure in *Pnma* were not successful.)

Data sets were collected on several different crystals. In each case the standards showed an exponential decrease in intensity with time. The standards of the various crystals studied decayed by 26–65% over the 3 days required to collect the data. A combination of two data sets was used in the final refinement of the structure. The data were corrected for the decay by using an anisotropic decay correction.[16] No absorption correction was made because of the small value of the absorption coefficient and the decay of the crystal during data collection. Crystal data and the details of data collection and reduction are given in Table I.

Determination and Refinement of the Structure

$Co(C_{10}H_8N_2)_3Cl_2\cdot 2H_2O\cdot C_2H_5O$ (1). The structure was solved by direct methods. The locations of the cobalt and five of the six nitrogens coordinated to it were found on an *E* map from MULTAN-78. A series of Fourier and difference Fourier maps[15] resulted in the location of the rest of the bipyridine ligands, three chloride ions and one water in special positions, and one chloride ion in a general position with half-occupancy along with another water and an ethanol molecule in general positions per asymmetric unit. The distance of 3.11 Å between two symmetry-related positions occupied by Cl4 is too short for a Cl–Cl contact.[17] This requires that the chloride be in one or the other position but not in both simultaneously. To allow for this, the occupancy factor for Cl4 was fixed at 0.5. However, after several cycles of full-matrix least-squares refinement,[18a] it was noted that Cl4 had very small thermal parameters and several peaks of ~1 e/Å^3 near it; this indicated the presence of more electron density than a chloride with an occupancy factor of 0.5 could account for. Since the occupancy factor of Cl4 could not be increased to account for this extra electron density and since the distance of 3.11 Å is ideal for an O–H···Cl[19] hydrogen bond, the model was modified by the

(14) $R_1 = \sum||F_o| - |F_c||/\sum|F_o|$; $R_2 = [\sum w(|F_o| - |F_c|)^2/\sum w|F_o|^2]^{1/2}$.
(15) Except where otherwise noted, all calculations were performed by using SHELX-76: Sheldrick, G. M. In "Computing in Crystallography"; Schenk H., Olthof-Hazekamp, R., van Koningsveld, H., Bassi, G. C., Eds.; Delft University Press: Delft, Holland, 1978; pp 34–42.
(16) Churchill, M. R.; Kalra, K. L. *Inorg. Chem.* **1974**, *13*, 1427.
(17) Pauling, L. "The Nature of the Chemical Bond"; Cornell University Press: Ithaca, NY, 1960; p 259.
(18) (a) Neutral-atom scattering factors were taken from: "International Tables for X-ray Crystallography"; Kynoch Press: Birmingham, England, 1974; Vol. IV, p 99. (b) Anomalous scattering factors were those of: Cromer, D. T.; Liberman, D. *J. Chem. Phys.* **1970**, *53*, 1891.

Table II. $Co(bpy)_3Cl_2 \cdot 2H_2O \cdot EtOH$ Atomic Coordinates[a]

atom	x	y	z
Co	−0.72702 (13)	−0.57813 (13)	−0.527 46 (2)
N1	−0.6214 (7)	−0.5286 (7)	−0.555 56 (11)
C12	−0.5561 (8)	−0.5770 (8)	−0.558 06 (14)
C13	−0.4797 (9)	−0.5478 (10)	−0.575 07 (16)
C14	−0.4731 (10)	−0.4685 (10)	−0.590 09 (16)
C15	−0.5398 (10)	−0.4216 (11)	−0.587 78 (16)
C16	−0.6122 (9)	−0.4517 (9)	−0.570 41 (15)
N2	−0.6459 (6)	−0.6796 (7)	−0.526 01 (12)
C22	−0.5696 (9)	−0.6642 (8)	−0.541 50 (15)
C23	−0.5120 (9)	−0.7235 (10)	−0.541 94 (17)
C24	−0.5300 (10)	−0.8027 (10)	−0.526 0 (2)
C25	−0.6065 (9)	−0.8183 (9)	−0.510 65 (18)
C26	−0.6628 (10)	−0.7573 (9)	−0.510 45 (16)
N3	−0.8049 (7)	−0.4790 (7)	−0.536 51 (12)
C32	−0.9026 (9)	−0.5349 (8)	−0.547 77 (15)
C33	−0.9631 (9)	−0.4803 (10)	−0.554 56 (16)
C34	−0.9185 (11)	−0.3650 (11)	−0.550 37 (18)
C35	−0.8143 (11)	−0.3046 (10)	−0.539 42 (17)
C36	−0.7632 (9)	−0.3687 (9)	−0.532 73 (16)
N4	−0.8806 (6)	−0.6980 (7)	−0.543 27 (12)
C42	−0.9455 (8)	−0.6587 (8)	−0.551 61 (14)
C43	−1.0457 (9)	−0.7278 (9)	−0.562 87 (16)
C44	−1.0812 (10)	−0.8417 (10)	−0.565 50 (16)
C45	−1.0152 (10)	−0.8841 (9)	−0.556 68 (16)
C46	−0.9185 (9)	−0.8121 (8)	−0.545 75 (15)
N5	−0.8049 (6)	−0.6248 (6)	−0.496 74 (11)
C52	−0.7467 (8)	−0.5482 (8)	−0.480 92 (14)
C53	−0.7864 (9)	−0.5653 (9)	−0.459 99 (15)
C54	−0.8892 (10)	−0.6639 (9)	−0.455 31 (17)
C55	−0.9465 (8)	−0.7437 (9)	−0.471 47 (16)
C56	−0.9021 (8)	−0.7193 (8)	−0.491 62 (15)
N6	−0.6037 (6)	−0.4446 (6)	−0.507 50 (12)
C62	−0.6373 (8)	−0.4453 (8)	−0.487 42 (14)
C63	−0.5716 (9)	−0.3526 (8)	−0.473 56 (16)
C64	−0.4728 (9)	−0.2600 (8)	−0.480 84 (17)
C65	−0.4365 (8)	−0.2607 (9)	−0.501 23 (19)
C66	−0.5028 (9)	−0.3535 (9)	−0.513 93 (17)
Cl1	−0.0564 (3)	0.0000	0.0000
Cl2	−0.7465 (3)	−0.37323 (15)	−0.0833
Cl3	−1.7303 (4)	−0.86513 (19)	−0.0833
Cl4	−0.5441 (4)	−0.4713 (4)	−0.187 98 (6)
O1	−0.8235 (8)	0 0000	0 0000
O2	−0.6954 (8)	−0.7358 (7)	−0.128 46 (12)
O3	−0.8917 (11)	−1.1082 (9)	−0.5394 (2)
C2	−0.822 (2)	−0.0262 (18)	−0.5524 (4)
C1	−0.7720 (15)	−0.0290 (18)	−0.5688 (3)
O4	−0.5441 (4)	−0.4713 (4)	−0.187 98 (6)

[a] Numbers in parentheses are errors in the last significant digit(s).

addition of a water molecule with an occupancy factor of 0.5 sharing the position occupied by Cl4.

Corrections for anomalous dispersion effects were included for all atoms.[18b] Anisotropic temperature factors were used for all non-hydrogen atoms. The locations of the hydrogen atoms on the bipyridine ligands were calculated (C–H bond length 0.95 Å), and the hydrogen atoms were allowed to "ride" on the atom to which they were attached. A common isotropic temperature factor for all these hydrogen atoms refined to a value $U = 0.069$ (7) Å^2. The hydrogen atoms on the solvent molecules were not located.

The quantity $\sum w(|F_o| - |F_c|)^2$ where $w = 0.9625(\sigma^2(F_o) + 0.002245F_o^2)$ was minimized in the least-squares refinement. During the final least-squares cycle the largest parameter shift was less than 0.04 of its standard deviation. The final R_1 value[14] was 0.056. The final weighted discrepancy index[14] R_2 was 0.066. For the enantiomorphic structure in $P6_122$ the final value for R_2 was 0.120, thus confirming the selection of $P6_522$ as the space group at the 99.5% significance level.[20]

The final non-hydrogen atomic positions are reported in Table II.

$Co(C_{10}H_8N_2)_3Cl \cdot H_2O$ (2). The position of the cobalt was calculated from a Patterson map. The locations of the chloride ion, the three bipyridine ligands, and the water of hydration were found in a series of difference Fourier maps.[15] The structure was initially refined with two data sets from two different crystals. Both refinements resulted in equivalent structures containing large standard deviations in the bond lengths and angles. The two data sets were then combined into one. This resulted in the structure reported here containing features equivalent to the ones observed in the separate refinements but with substantially smaller standard deviations. Anisotropic temperature factors were used only for the cobalt, chloride, and oxygen due to the limited number of data. The hydrogen atoms were treated in the same manner as previously described. The common temperature factor for the hydrogens refined to a value $U = 0.10$ (1) Å^2.

Table III. $Co(bpy)_3Cl \cdot H_2O$ Atomic Coordinates[a]

atom	x	y	z
Co	−0.1131 (3)	−0.07502 (12)	0.0000
Cl	−0.2957 (7)	−0.2185 (3)	−0.5017 (7)
N1	−0.2909 (19)	−0.1110 (8)	−0.0727 (13)
C12	−0.267 (2)	−0.1456 (9)	−0.1622 (17)
C13	−0.377 (3)	−0.1777 (13)	−0.203 (2)
C14	−0.500 (3)	−0.1737 (11)	−0.168 (2)
C15	−0.526 (3)	−0.1395 (10)	−0.0813 (18)
C16	−0.418 (2)	−0.1090 (9)	−0.0370 (16)
N2	−0.036 (2)	−0.1118 (8)	−0.1366 (14)
C22	−0.125 (3)	−0.1440 (11)	−0.1914 (18)
C23	−0.084 (3)	−0.1763 (11)	−0.2833 (19)
C24	0.053 (3)	−0.1704 (11)	−0.3100 (19)
C25	0.147 (2)	−0.1354 (11)	−0.2569 (18)
C26	0.093 (3)	−0.1081 (11)	−0.1669 (18)
N3	−0.2174 (19)	−0.0566 (7)	0.1387 (13)
C32	−0.225 (2)	−0.1043 (9)	0.2063 (16)
C33	−0.301 (3)	−0.0999 (11)	0.2983 (20)
C34	−0.375 (3)	−0.0470 (13)	0.318 (2)
C35	−0.363 (3)	0.0010 (13)	0.2512 (20)
C36	−0.288 (2)	−0.0047 (11)	0.1577 (19)
N4	−0.0782 (17)	−0.1549 (7)	0.0872 (12)
C42	−0.147 (3)	−0.1579 (12)	0.1819 (20)
C43	−0.127 (3)	−0.2096 (12)	0.244 (2)
C44	−0.042 (3)	−0.2562 (13)	0.215 (2)
C45	0.021 (3)	−0.2550 (12)	0.1227 (19)
C46	0.006 (2)	−0.2031 (10)	0.0602 (20)
N5	0.0766 (17)	−0.0321 (7)	0.0467 (13)
C52	0.088 (2)	0.0293 (9)	0.0230 (17)
C53	0.207 (2)	0.0601 (10)	0.0513 (16)
C54	0.312 (3)	0.0339 (13)	0.102 (2)
C55	0.302 (3)	−0.0287 (11)	0.1248 (20)
C56	0.182 (3)	−0.0589 (11)	0.0975 (18)
N6	−0.1338 (20)	0.0167 (7)	−0.0533 (13)
C62	−0.024 (3)	0.0529 (9)	−0.0318 (15)
C63	−0.031 (3)	0.1183 (11)	−0.0617 (18)
C64	−0.145 (3)	0.1367 (12)	−0.1115 (20)
C65	−0.254 (3)	0.1007 (10)	−0.1374 (19)
C66	−0.243 (3)	0.0391 (11)	−0.1028 (18)
O1	0.586 (2)	0.1665 (11)	0.0708 (18)

[a] Numbers in parentheses are errors in the last significant digit(s).

After several more cycles of least-squares refinement minimizing the function $\sum w(|F_o| - |F_c|)^2$ where $w = 1.8858/(\sigma^2(F_o) + 0.001959F_o^2)$, the refinement was terminated when the parameter shifts became less than 0.02 of their standard deviation. The final R_1 value was 0.084 and the final weighted discrepancy index R_2 was 0.085. The Hamilton R-factor test at the end of refinement confirmed the choice of the hand of the molecule at the 99.5% significance level.

A final difference Fourier map revealed no peak greater than ±0.5 e/Å^3, about the size of a hydrogen atom. The final non-hydrogen atomic positions are reported in Table III.

Results and Discussion

Description of Structures. A view of the $Co(bpy)_3^{2+}$ ion in **1** and the atom-labeling scheme used are shown in Figure 1. The interatomic distances and angles with their standard deviations are contained in Tables IV and S1 (Table S1 is supplementary material). The thermal parameters for the non-hydrogen atoms and the positional parameters for the hydrogen atoms are given in Tables S2 and S3, respectively, (supplementary material). A listing of the final observed and calculated structure factor amplitudes can be found in Table

(19) (a) Templeton, D. H.; Zalkin, A.; Ruben, H. W.; Templeton, L. K. *Acta Crystallogr., Sect. B* **1979**, *B35*, 1608. (b) Taylor, R.; Kennard, O. *J. Am. Chem. Soc.* **1982**, *104*, 5063.
(20) Hamilton, W. C. *Acta Crystallogr.* **1965**, *18*, 502.

Table IV. Bond Distances (Å) and Angles (deg) for $Co(bpy)_3Cl_2 \cdot 2H_2O \cdot EtOH$[a]

Cobalt–Ligand Distances

Co–N1	2.141 (7)	Co–N3	2.133 (7)	Co–N5	2.125 (7)
Co–N2	2.123 (7)	Co–N4	2.117 (8)	Co–N6	2.128 (7)

Cobalt–Ligand Angles

N1–Co–N2	76.3 (3)	N1–Co–N6	96.1 (3)	N2–Co–N6	94.7 (3)	N4–Co–N5	92.9 (3)
N1–Co–N3	92.4 (3)	N2–Co–N3	167.1 (3)	N3–Co–N4	75.9 (3)	N4–Co–N5	164.2 (3)
N1–Co–N4	95.3 (3)	N2–Co–N4	98.5 (3)	N3–Co–N5	95.8 (3)	N5–Co–N6	77.2 (3)
N1–Co–N5	169.5 (3)	N2–Co–N5	96.1 (3)	N3–Co–N6	92.7 (3)		

2,2′-Bipyridine Distances

	X					
	1	2	3	4	5	6
N(*X*)–C(*X*2)	1.33 (1)	1.35 (1)	1.34 (1)	1.33 (1)	1.36 (1)	1.33 (1)
N(*X*)–C(*X*6)	1.34 (1)	1.36 (1)	1.31 (1)	1.36 (1)	1.32 (1)	1.35 (1)
C(*X*2)–C(*X*3)	1.39 (1)	1.36 (1)	1.40 (1)	1.38 (1)	1.39 (1)	1.40 (1)
C(*X*3)–C(*X*4)	1.39 (1)	1.38 (1)	1.37 (1)	1.36 (1)	1.38 (1)	1.36 (1)
C(*X*4)–C(*X*5)	1.33 (2)	1.34 (1)	1.39 (2)	1.38 (1)	1.39 (1)	1.36 (1)
C(*X*5)–C(*X*6)	1.37 (1)	1.36 (1)	1.40 (1)	1.35 (1)	1.36 (1)	1.36 (1)
C(12)–C(22)	1.50 (1)	C(32)–C(42)	1.48 (1)	C(52)–C(62)	1.48 (1)	

[a] Numbers in parentheses are errors in last significant digit(s).

Table V. Bond Distances (Å) and Angles (deg) for $Co(bpy)_3Cl \cdot H_2O$[a]

Cobalt–Ligand Distances

Co–N1	2.119 (18)	Co–N3	2.113 (17)	Co–N5	2.152 (16)
Co–N2	2.091 (18)	Co–N4	2.099 (15)	Co–N6	2.114 (16)

Cobalt–Ligand Angles

N1–Co–N2	76.6 (7)	N1–Co–N6	96.9 (7)	N2–Co–N6	96.3 (7)	N4–Co–N5	93.7 (6)
N1–Co–N3	93.6 (7)	N2–Co–N3	166.9 (7)	N3–Co–N4	76.6 (6)	N4–Co–N6	165.6 (7)
N1–Co–N4	94.1 (6)	N2–Co–N4	95.3 (7)	N3–Co–N5	94.9 (6)	N5–Co–N6	76.6 (7)
N1–Co–N5	169.6 (7)	N2–Co–N5	95.8 (7)	N3–Co–N6	93.4 (6)		

2,2′-Bipyridine Distances

	X					
	1	2	3	4	5	6
N(*X*)–C(*X*2)	1.41 (2)	1.32 (3)	1.36 (2)	1.41 (3)	1.37 (2)	1.35 (2)
N(*X*)–C(*X*6)	1.32 (2)	1.32 (3)	1.34 (2)	1.37 (2)	1.35 (3)	1.33 (3)
C(*X*2)–C(*X*3)	1.38 (3)	1.44 (3)	1.42 (3)	1.40 (3)	1.39 (3)	1.47 (3)
C(*X*3)–C(*X*4)	1.28 (4)	1.38 (3)	1.38 (3)	1.36 (3)	1.34 (3)	1.35 (3)
C(*X*4)–C(*X*5)	1.37 (3)	1.37 (3)	1.36 (3)	1.36 (3)	1.39 (3)	1.36 (3)
C(*X*5)–C(*X*6)	1.37 (3)	1.42 (3)	1.43 (3)	1.40 (3)	1.39 (3)	1.41 (3)
C(12)–C(22)	1.44 (3)	C(32)–C(42)	1.42 (3)	C(52)–C(62)	1.40 (2)	

[a] Numbers in parentheses are errors in the last significant digit(s).

S4 (supplementary material). The six coordinated nitrogen atoms of the three 2,2′-bipyridine ligands form a distorted octahedron about the Co^{2+} ion. The average Co–N bond distance is 2.128 (8) Å with an average N–Co–N "bite" angle of 76.5 (8)°. The average C–C and C–N bond lengths within the 2,2′-bipyridine groups are 1.37 (2) (bridging C–C = 1.49 (1) Å) and 1.34 (2) Å, respectively. The maximum deviation from the best plane within the pyridine rings is ±0.019 Å, and the average angle between the two pyridines of a bipyridine is 3.6°.

The numbering scheme used for the atoms in the cobalt(I) complex **2** is identical with that used for $Co(bpy)_3^{2+}$ (Figure 1). The interatomic bond distances and angles for **2** are listed with their standard deviations in Tables V and S5 (Table S5 is supplementary material) and the thermal parameters for the non-hydrogen atoms and the hydrogen atom positional parameters are available as Tables S6 and S7, respectively (supplementary material). A listing of the final observed and calculated structure factor amplitudes is given in Table S8 (supplementary material).

The cobalt(I) in **2** is six-coordinate with its coordination sphere being the six nitrogen atoms of the three bipyridine ligands. The coordination geometry is a distorted octahedron with the bond distances and angles in the coordination sphere being nearly identical with those found in $Co(bpy)_3^{2+}$. The

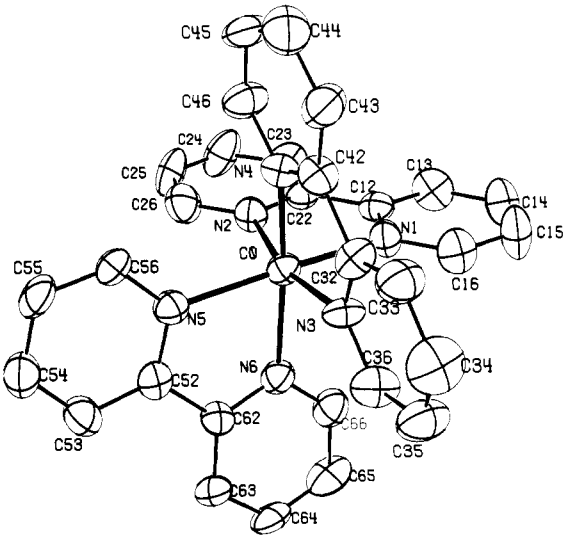

Figure 1. ORTEP drawing of the $Co(bpy)_3^{2+}$ cation with thermal ellipsoids at the 50% probability level. The atom-numbering scheme used is shown.

average Co–N bond length is 2.11 (2) Å, and the average N–Co–N "bite" angle is 76.6 (7)°. (Note that the relatively

Table VI. Hydrogen Bonding in $Co(bpy)_3Cl_2$

	H-A, Å	D-A, Å	D-H-A, deg
O1···Cl1[a]		3.118	
O2···O1[b]		2.830	
O2···Cl3[c]		3.219	
O3···Cl1[d]		3.107	
O4···Cl4[e]		3.155	
O4···O2[e]		3.000	
H53···Cl2[f]	2.66	3.61	175
H63···Cl2[f]	2.68	3.61	168
H13···Cl2[g]	2.78	3.71	166
H33···Cl2[h]	2.87	3.82	173
H43···Cl2[h]	2.93	3.87	171
H23···Cl2[g]	3.05	3.98	168

[a] $-1+x, y, z$. [b] $x-y, x, -0.166667+z$. [c] $1+x, y, z$. [d] $-1-x, -1-y, -0.5+z$. [e] $y, x, -0.33333-z$. [f] $-1-y, x-y, -0.33333+z$. [g] $-1-x, -1-y, -0.5+z$. [h] $-2-x, -1-y, -0.5+z$.

low accuracy of this structure determination, due to the problem of crystal decay and the lack of high-angle data, makes a comparison of the average values of chemically equivalent bonds more meaningful than the individual values.) The greatest difference between the $Co(bpy)_3^{2+}$ and $Co(bpy)_3^{+}$ structures is within the bipyridine ligands: In the Co(I) complex the average bridging C–C′ bond length is 1.42 (2) Å, ~0.07 (2) Å shorter than that in **1**; the C–N and other C–C bonds (average 1.35 (3) and 1.38 (4) Å, respectively) do not differ significantly from those in **1**.

The maximum deviation from the best plane within the pyridine rings is ±0.03 Å, and the average angle between the planes of the two pyridine rings of a bpy is 3.0°.

Hydrogen Bonding. $Co(bpy)_3Cl_2·2H_2O·EtOH$. A view of the crystal packing and hydrogen bonding is provided in Figure S1 (supplementary material), and parameters relevant to the hydrogen bonding are given in Table VI. The waters and ethanol of crystallization are involved in a hydrogen-bonding network with each other and with three of the four chlorides in the asymmetric unit. The remaining chloride ion is not involved in hydrogen bonding to the solvent molecules but is surrounded by twelve hydrogen atoms (H3 and H3′) of the bipyridine ring. The H···Cl distances range from 2.66 to 3.05 Å and the C–H···Cl angles from 166 to 175° (Table VI). As is shown in Figure S2 (supplementary material), the twelve hydrogen bonds involving H3 and H3′ are arranged in an approximate dodecahedron about the chloride. Although the hydrogen atoms bound to a carbon α to a nitrogen are the most likely to engage in C–H···X hydrogen bonding,[19b] the 3, 3′ protons of 2,2′-bipyridine (β to nitrogen) have been determined to be the most acidic protons on the ring.[21] The acidity of these protons combined with the H···Cl distances and the linearity of the C–H···Cl bond strongly suggests that these are C–H···Cl hydrogen bonds.[19,22] Hydrogen bonding involving the H3 and H3′ protons has been observed in $Ir(bpy)_3^{3+}$ [21,23] as well, but was attributed[23] to N–H···X hydrogen bonding.

$Co(bpy)_3Cl·H_2O$. The unit cell and the hydrogen bonding in $Co(bpy)_3Cl·H_2O$ can be viewed in Figure S3 (supplementary material), and details of the bonding are presented in Table VII. The water of crystallization is involved in hydrogen bonds with the chloride ion with a Cl···O···Cl angle of 101° (Table VII). As is shown in Figure S4 (supplementary material), this chloride ion is also involved in five C–H···Cl hydrogen bonds involving H3 and H3′ protons of the bipyridine,

Table VII. Hydrogen Bonding in $Co(bpy)_3Cl$

	H-A, Å	D-A, Å	D-H-A, deg
O1···Cl[a]		3.18	*f*
O1···Cl[b]		3.36	*f*
H23···Cl[c]	2.8	3.63	151
H24···Cl[d]	2.8	3.77	164
H33···Cl[e]	2.7	3.66	174
H43···Cl[e]	2.8	3.70	179
H53···Cl[a]	2.7	3.60	167
H63···Cl[a]	3.0	3.92	172

[a] $-x, -y, 1/2+z$. [b] $1/2-x, 1/2+y, 1/2+z$. [c] x, y, z. [d] $-1/2+x, 1/2+y+z$. [e] $x, y, 1+z$. [f] Cl-O1-Cl = 101°.

like the ones described previously in $Co(bpy)_3^{2+}$. The dodecahedral arrangement of hydrogen bonds observed for **1** is partially disrupted here with some of the weaker C–H···Cl hydrogen bonds replaced by stronger O–H···Cl hydrogen bonds. There is also one possible "hydrogen bond" involving an H4 proton. However, it is not clear whether this is a true hydrogen bond or an artifact due to crystal-packing forces and the hydrogen bonding of the H3 proton to a symmetry-related chloride ion.

Comparison with Related Complexes. 2,2′-Bipyridine complexes of most metals are known, and an extensive data base for the tris chelates is available.[24] Included are a number of "normal" complexes, e.g. $Ni(bpy)_3^{2+}$ and $Co(bpy)_3^{2+}$, whose chemical, spectral, and magnetic properties resemble those of the corresponding metal–amine or metal–aquo complexes. For others, especially those containing the d^6 metal centers Fe(II), Ru(II), and Os(II), the π-acceptor ability of 2,2′-bipyridine leads to enhanced stability, to intense metal-to-ligand charge-transfer absorption, and, for Fe(II), to the low-spin d^6 configuration, which maximizes the π-back-bonding interaction. In addition, 2,2′-bipyridine stabilizes low oxidation states, and an extraordinary series of $M(bpy)_3^n$ (n = 1+, 0, and 1−) compounds exists. The electronic, vibrational, and EPR spectra of a number of the latter implicate the presence of the bpy^- group[24-26] in which essentially complete transfer of one electron from the metal center to the bound bpy has occurred. Finally, there are "intermediate" species in which transfer of charge to the bpy appears substantial but not complete. On the basis of IR and other data, Saito et al.[26] have suggested that $Cr(bpy)_3^{2+}$ and $Co(bpy)_3^{+}$ are of the intermediate type.

The accumulation of negative charge on 2,2′-bipyridine is predicted[27] to lead to an increased bond order at the bridging C–C′ position and to changes in the intrapyridine bond lengths as shown in

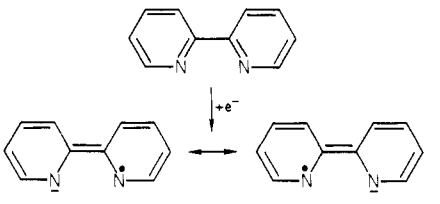

These skeletal shifts are experimentally observed as lowered intra-pyridine C–C and C–N infrared[26] and Raman and resonance-Raman stretching frequencies,[28,29] and in two recent

(21) Constable, E. C.; Seddon, K. R. *J. Chem. Soc., Chem. Commun.* **1982**, 34.
(22) Hamilton, W. C.; Ibers, J. A. "Hydrogen Bonding in Solids"; W. A. Benjamin: New York, 1968.
(23) Wickramasinghe, W. A.; Bird, P. H.; Serpone, N. *J. Chem. Soc., Chem. Commun.* **1981**, 1284.
(24) (a) McWhinnie, W. R.; Miller, J. D. *Adv. Inorg. Chem. Radiochem.* **1969**, *12*, 135. (b) McKenzie, E. D. *Coord. Chem. Rev.* **1971**, *6*, 187.
(25) See the following and references cited therein: (a) Creutz, C. *Comments Inorg. Chem.* **1982**, *1*, 293. (b) Heath, G. A.; Yellowlees, L. J.; Braterman, P. S. *J. Chem. Soc., Chem. Commun.* **1981**, 287. (c) Motten, A. G.; Hanck, K.; DeArmond, M. K. *Chem. Phys. Lett.* **1981**, *79*, 541. (d) Saji, T.; Aoyaguii, S. *J. Electroanal. Chem.* **1975**, *63*, 31. (e) Hanazaki, I.; Nagakura, S. *Bull. Chem. Soc. Jpn.* **1971**, *44*, 2312. (f) Koenig, E.; Herzog, S. *J. Inorg. Nucl. Chem.* **1970**, *32*, 585, 601, 613.
(26) Saito, Y.; Takemoto, J.; Hutchinson, B.; Nakamoto, K. *Inorg. Chem.* **1972**, *11*, 2003.
(27) Takahashi, C.; Maeda, S. *Chem. Phys. Lett.* **1974**, *24*, 584.

Table VIII. Structural and Spectral Data for 2,2′-Bipyridine Complexes[a]

		M–N, Å	N–M–N, deg	C–C′, Å	ref	ν(bpy), cm⁻¹ [b]			ν(M–N),[b] cm⁻¹
$Fe(bpy)_3^{3+}$	$(\pi d)^5$	1.963	82.3		32	1609	1570		384, 367
$Co(bpy)_3^{3+}$	$(\pi d)^6$	1.93 (2)	83.3 (5)	1.45 (2)	33	1610	1575		378, 370
$Rh(bpy)_3^{3+}$ [c]	$(\pi d)^6$	2.038 (5)	80.2 (2)	1.469 (9)	31				
$Fe(bpy)_3^{2+}$	$(\pi d)^6$	1.97 (1)[b]			5	1609	1570		386, 376[d]
$Ru(bpy)_3^{2+}$	$(\pi d)^6$	2.056	78.7	1.476	34				338, 326[e]
$Co(bpy)_3^{2+}$	$(\pi d)^5(\sigma d)^2$	2.128 (8)	76.5 (8)	1.49 (1)		1600	1575		266, 248
$Ni(bpy)_3^{2+}$	$(\pi d)^6(\sigma d)^2$	2.089 (9)	78.6 (3)	1.48 (1)	35				282, 258
$Co(bpy)_3^{+}$	$(\pi d)^6(\sigma d)^2$	2.11 (2)	76.6 (7)	1.42 (2)		1590	1565	970	238, 185
$Cu(bpy)_3^{2+}$	$(\pi d)^6(\sigma d)^3$	2.031 (14)[f] 2.34 (16)[f]	73.9–80.4	1.48 (2)	36	1605	1580		291, 268
$Mo(O\text{-}i\text{-}Pr)_2(bpy)_2$	d^3	2.118 (8)	73.6 (4)	1.424 (1)	29				
Fe(η^6-tol)bpy	d^8	1.902 (1)	81.9 (1)	1.417 (3)	30	1582	1515		
bpy				1.490 (3)	29	1582	1560[g]		
Li^+bpy^-						~1580	1500	944	

[a] Numbers in parentheses are errors in the last significant digit(s). [b] Data taken from ref 26. [c] The complex is tris(3,3′-dimethyl-2,2′-bipyridine)rhodium(III). [d] Data for $Fe(phen)_3^{2+}$. [e] From ref 37a. [f] The Cu(I) complex is distorted. The first distance is the average over the four short bonds and the second value is the average of the two long bonds. [g] Reference 37b.

papers[29,30] the shortening of the bridging carbon–carbon bond has been directly observed with via X-ray diffraction studies of the crystals.

In order to compare the results obtained here for $Co(bpy)_3^{2+}$ and $Co(bpy)_3^{+}$ with the properties of related complexes, we present electronic configurations, bond parameters, and infrared data for bpy, bpy^-, and a number of bpy complexes in Table VIII. Since we wish to conserve space and because the largest changes are observed in the C–C′ bridging bond of bpy, only intra-bpy bond distances for the latter are included.

The average N–M–N bite angles found for $Co(bpy)_3^{2+}$ and $Co(bpy)_3^{+}$ are consistent with the trend toward decreasing bite angles with increasing M–N bond lengths. The latter in turn reflect the role of electrostatic and electronic factors. The values of d_{M-N} for first-transition-series complexes cluster about 1.95 Å for complexes of trivalent metals and around 2.1 Å for those of divalent metals. (Note the concomitant shift in infrared metal–nitrogen stretching frequencies; far right of Table VIII.) In addition specific electronic effects are evident: the nearly identical Fe–N bond distances for the Fe(II) and Fe(III) complexes mentioned earlier are attributed, in part, to Fe(II)-to-bpy back-donation, and comparison of the $Co(bpy)_3^{2+}$–$Co(bpy)_3^{+}$ data shows that such effects are comparable for high-spin d^7–d^8 couples.

The bridging C–C′ bond length in bpy, 1.490 (3) Å, is altered little in most of the known tris(bipyridine) complexes, and the length determined here for $Co(bpy)_3^{2+}$, 1.49 (1) Å, appears quite normal. By contrast, the recent structural studies of $Mo(O\text{-}i\text{-}Pr)_3(bpy)_2$[29] and Fe($\eta^6$-tol)bpy (tol = $C_6H_5CH_3$)[30] revealed extremely short (~1.42 Å) C–C′ bonds as well as a lengthening of the intra-pyridine C–N bonds (compared to bpy). As discussed above, bonding changes of this nature are expected when bpy is reduced to bpy^-. In accord with this interpretation, the resonance-Raman or IR spectra of these compounds contain bipyridine bands shifted toward those of bpy^-. The C–C′ bond length found here for $Co(bpy)_3^{+}$ is 1.42 (2) Å. Although the $Co(bpy)_3^{+}$ structure is not a very accurate one, the fact that $Co(bpy)_3^{+}$ also exhibits bpy^--like IR spectral features suggests that this apparent bond shortening may be real. If it is real, it implies substantial Co(I)-to-bpy charge transfer, presumably via $\pi d \rightarrow$ bpy π^* back-donation. This interaction is favored for $Co(bpy)_3^{+}$ more than for any of the other $M(bpy)_3$ complexes tabulated because its πd and bpy π^* levels lie closer in energy.[38] The structures and other physical properties of $Co(bpy)_3^{+}$ and related complexes clearly merit further investigation. Confirmation of large intraligand structural changes would be especially desirable. In addition, it is of some interest to clarify the role of the unpaired σ^*d electrons in determining the bonding and spectral properties.

In regard to the $Co(bpy)_3^{n+}$ bond lengths, the M–N bond length difference (Δd_0) for Co(II)–Co(III) is 0.20 Å, similar to the values 0.19 Å for $Co(phen)_3^{3+/2+}$ and 0.22 Å for $Co(NH_3)_6^{3+/2+}$, both of which were recently determined directly by EXAFS analysis,[3] and $Co(NH_3)_6^{3+/2+}$ values obtained through X-ray crystallography: $Co(NH_3)_6^{2+}$, 2.16 Å;[39] $Co(NH_3)_6^{3+}$, 1.965 (1) Å;[40] Δd_0 = 0.19 Å. Few appropriate comparisons for $Co(bpy)_3^{+}$ exist since coordination number 6 is extremely rare for Co(I), but in (usually low-spin) five-coordinate Co(I) complexes the Co(I)–N bands are generally much shorter than those found here (2.11 Å): In the complex (2,2′,2″-terpyridine)tetrahydroborato-*H*,*H*′)cobalt(I),[41] the Co(I)–N(outer) bond distance is 1.926 (3) Å and in $Co(CH_3CN)(C_2H_4)(P(CH_3)_3)_3^{+}$ the Co(I)–N bond length is 1.913 (6) Å.[42] In the six-coordinate species (2,6-diacetyl-

(28) (a) Dallinger, R. F.; Woodruff, W. H. *J. Am. Chem. Soc.* **1979**, *101*, 4393. (b) Bradley, P. G.; Kress, N.; Hornberger, B. A.; Dallinger, R. F.; Woodruff, W. H. *Ibid.* **1981**, *103*, 7441.
(29) Chisholm, M. H.; Huffman, J. C.; Rothwell, I. P.; Bradley, P. G.; Kress, N.; Woodruff, W. H. *J. Am. Chem. Soc.* **1981**, *103*, 4945.
(30) Radonovich, L. J.; Eyring, M. W.; Groshens, T. J.; Klabunde, K. J. *J. Am. Chem. Soc.* **1982**, *104*, 2816.
(31) Ohba, S.; Miyamae, H.; Sato, S.; Saito, Y. *Acta Crystallogr., Sect. B* **1979**, *B35*, 1470.
(32) Figgis, B. N.; Skelton, B. W.; White, A. H. *Aust. J. Chem.* **1978**, *31*, 57.
(33) Yanagi, K.; Ohashi, Y.; Sasada, Y.; Kaizu, Y.; Kobayashi, H. *Bull. Chem. Soc. Jpn.* **1981**, *54*, 118.
(34) Rillema, D. P.; Jones, O. S.; Levy, H. A. *J. Chem. Soc., Chem. Commun.* **1979**, 849
(35) Wada, A.; Sakabe, N.; Tanaka, J. *Acta Crystallogr., Sect. B* 1976, *B32*, 1121. Wada, A.; Katayama, C.; Tanaka, J. *Ibid.* **1976**, *B32*, 3194.
(36) Anderson, O. P. *J. Chem. Soc., Dalton Trans.* **1973**, 2597.
(37) (a) Staniewicz, R. J.; Hendricker, D. G.; Griffiths, P. R. *Inorg. Nucl. Chem. Lett.* **1977**, *13*, 467. (b) Inskeep, R. G. *J. Inorg. Nucl. Chem.* **1962**, *24*, 763.
(38) This can be seen qualitatively through the following comparisons: For $Fe(bpy)_3^{2+}$ and $Ru(bpy)_3^{2+}$, for which back-donation is an important bonding component, the lowest metal-to-ligand charge-transfer absorptions fall in the visible region (510 and 450 nm, respectively). For $Co(bpy)_3^{+}$ the lowest energy transition occurs in the near-infrared (1390 nm).[11] With all these assumed to be $\pi d \rightarrow$ bpy π^* transitions (for $Co(bpy)_3^{+}$, $\sigma^*d \rightarrow$ bpy π^* is also possible but such a transition has never been observed), the $\pi d \rightarrow$ bpy π^* orbitals lie ~1.6 eV closer in $Co(bpy)_3^{+}$ than in $Fe(bpy)_3^{2+}$ or $Ru(bpy)_3^{2+}$. It is noteworthy, however, that although the energetics favor greater mixing (delocalization) for $Co(bpy)_3^{+}$, analysis of the MLCT band intensities (for the details and for the Fe(II) and Ru(II) spectra cited above, see: Mason, S. F. *Inorg. Chim. Acta, Rev.* **1968**, *89*) gives the extent of transfer from M to bpy as 0.13 e for Ru(II), 0.055 e for Fe(II), and 0.051 e for Co(I). These results suggest that delocalization may be no greater for $Co(bpy)_3^{+}$ than for $Fe(bpy)_3^{2+}$.
(39) Freeman, H. C., unpublished results.
(40) Beattie, J. K.; Moore, C. J. *Inorg. Chem.* **1982**, *21*, 1292.
(41) Corey, E. J.; Copper, N. J.; Canning, W. M.; Lipscomb, W. N.; Koetzle T. F. *Inorg. Chem.* **1982**, *21*, 192.

pyridine *N,N'*-dimethyl-1,10-phenanthroline-2,9-diyl-hydrazone)(trimethyl phosphite)cobalt(I) the Co–N(phen) bond lengths are 2.124 (5) and 2.149 (5) Å, comparable to the Co–N(bpy) bond length in the present system.[43]

The tris(bipyridine) complexes are the only ones common to all three cobalt oxidation states. In these it is seen that the greatest metal–ligand-bonding changes occur when cobalt(III) is reduced to cobalt(II); not only does the positive charge on the metal decrease in this reduction but *two* σd electrons are "added" as well since the Co(II) complex is high spin. By contrast, negligible metal–ligand bond length changes occur when $Co(bpy)_3^{2+}$ is reduced to $Co(bpy)_3^{+}$; from the present work $\Delta d_0 = -0.02$ (2) Å and from EXAFS studies[3] $\Delta d_0 = -0.02$ (1) Å. As discussed above, this is attributed to the fact that the added electron enters a πd orbital and so is partially delocalized onto the π-acceptor bpy.

Barriers to Outer-Sphere Electron-Transfer Reactions. The rate constant k for an electron-exchange reaction such as

$$M(bpy)_3^{+} + M(bpy)_3^{2+} \rightleftharpoons M(bpy)_3^{2+} + M(bpy)_3^{+} \quad (1)$$

may be formulated[4,44] as the product of a preequilibrium constant K_A, an effective nuclear frequency ν_n, and electronic and nuclear factors κ_{el} and κ_n, respectively:

$$k = K_A \nu_n \kappa_{el} \kappa_n \quad (2)$$

Electron transfer is most probable when the reactants are brought into close proximity; K_A is the equilibrium constant for the formation of the precursor complex from the separated reactants

$$M(bpy)_3^{+} + M(bpy)_3^{2+} \rightleftharpoons M(bpy)_3^{+}\cdots M(bpy)_3^{2+} \quad (3)$$

and can be evaluated from

$$K_A = \frac{4\pi N r^2\, \delta r}{1000} \exp\left(-\frac{w(r)}{RT}\right) \quad (4)$$

where the reaction thickness δr is typically ca. 0.8 Å and $w(r)$ is the work required to bring the reactants to the separation distance r.[44] For tris(2,2'-bipyridine) couples K_A ranges from $\sim$0.3 to $\sim$1 M^{-1} depending upon charge type and the ionic strength of the medium (see ref 3 and references cited therein). For exchange reactions, the nuclear factor contains only solvent and inner-sphere contributions:

$$\kappa_n = \Gamma_\lambda \exp[-(\Delta G^*_{out} + \Delta G^*_{in})/RT] \quad (5)$$

where Γ_λ is the inner-sphere nuclear tunneling factor.[45] For $M(bpy)_3^{3+/2+}$, $M(bpy)_3^{2+/+}$, etc. couples ΔG^*_{out} is estimated as 3.3 kcal mol^{-1} in water[3] while ΔG^*_{in} depends on the couple and is given by

$$\Delta G^*_{in} = \tfrac{1}{2}\sum f_i((\Delta d_0)_i/2)^2 \quad (6)$$

where f_i is the reduced force constant for the ith inner-sphere vibration and is defined in terms of the normal mode force constants for that vibration, $f_i = 2f_{ox}f_{red}/(f_{ox} + f_{red})$, $(\Delta d_0)_i$ is the bond length difference for bond i in the two oxidation states $(\Delta d_0)_i = (d_{red} - d_{ox})_i$, and the sum is taken over all the intramolecular vibrations. The nuclear frequency appearing in eq 2 is related to the solvent and inner-sphere frequencies by

$$\nu_n^2 = \frac{\nu_{out}^2 \Delta G^*_{out} + \nu_{in}^2 \Delta G^*_{in}}{\Delta G^*_{out} + \Delta G^*_{in}} \quad (7)$$

For water as solvent $\nu_{out} \simeq 0.9 \times 10^{12}$ s^{-1} while metal–ligand and intraligand stretching frequencies are typically (9–15) $\times$ 10^{12} and (3–9) $\times$ 10^{13} s^{-1}, respectively.

Table IX. Comparison of Parameters for the $Co(bpy)_3^{3+}$–$Co(bpy)_3^{2+}$ and $Co(bpy)_3^{2+}$–$Co(bpy)_3^{+}$ Exchange Reactions in Water at 25 °C[a]

	$Co(bpy)_3^{3+/2+}$	$Co(bpy)_3^{2+/+}$
k_{obsd}, M^{-1} s^{-1}	18	10^9
K_A, M^{-1}	0.33	0.83
ΔG^*_{out}, kcal mol^{-1}	3.3	3.3
ΔG^*_{in}, kcal mol^{-1}	13.2 ± 1.4	0.1 [3 ± 1]
κ_n	10^{-11}–10^{-13}	3×10^{-3} [(0.4–14) $\times 10^{-5}$]
ν_n, s^{-1} [b]	1.2×10^{13}	0.5×10^{13} [2.7×10^{13}]
Γ_λ	5.0	1.0 [1.3]
k_{calcd}/κ_{el}, M^{-1} s^{-1}	2–200	2×10^{10} [>(0.1–3) $\times 10^9$]

[a] The values for the $Co(bpy)_3^{2+/+}$ exchange in square brackets include estimated contributions from the intraligand changes. [b] Note that eq 7, which was used in calculating the effective nuclear frequency ν_n, is only valid when all the relevant frequencies are low, i.e., $h\nu_i < 4kT$ (that is, less than 800 cm^{-1} at room temperature).

The results of this study bear on the electron-exchange barriers for two systems, the $Co(bpy)_3^{3+}$–$Co(bpy)_3^{2+}$ couple and the $Co(bpy)_3^{2+}$–$Co(bpy)_3^{+}$ couple. The exchange rate constant for $Co(bpy)_3^{3+}$–$Co(bpy)_3^{2+}$ is 18 M^{-1} s^{-1} at 25 °C and 0.1 M ionic strength,[46] while that for $Co(bpy)_3^{2+}$–$Co(bpy)_3^{+}$ is estimated at $\sim 10^9$ M^{-1} s^{-1} at 25 °C and 0.5 M ionic strength.[3,47] As mentioned above, the outer-sphere barriers for the two are comparable, $\Delta G^*_{out} = 3.3$ kcal mol^{-1}, but K_A for the $Co(bpy)_3^{2+}$–$Co(bpy)_3^{+}$ ($K_A \sim 0.83$ M^{-1}) is somewhat larger than that for the $Co(bpy)_3^{3+}$–$Co(bpy)_3^{2+}$ couple (0.33 M^{-1}).[3] Earlier EXAFS work[3] and the present work show that Δd_0 for the metal–nitrogen bonds is very large for the Co(II)–Co(II) couple (0.19 (2) Å) and very small for the Co(I)–Co(I) couple (from EXAFS –0.02 (1) Å and from the present work –0.02 (2) Å). Taking the force constants for the cobalt–nitrogen bonds[3] as 1.7×10^5 dyn cm^{-1} (the value for the $Co(NH_3)_6^{3+}$–$Co(NH_3)_6^{2+}$ couple; this assumption is made because the force constants for bidentate bpy complexes are not known) and including only metal–nitrogen bonds, we obtain ΔG^*_{in} values of 13.2 ± 1.4 and 0.1 kcal mol^{-1} for the $Co(bpy)_3^{3+}$–$Co(bpy)_3^{2+}$ and $Co(bpy)_3^{2+}$–$Co(bpy)_3^{+}$ exchanges, respectively. (The uncertainty given for the Co(III)–Co(II) couple arises only from an uncertainty of ±0.01 Å in Δd_0). In addition, although the errors are large for the $Co(bpy)_3^{+}$ structure, the C–C' bond in **2** appears significantly shorter than that in the Co(II) complex **1**, suggesting that $\Delta d_0 \sim 0.07$ (2) Å for the inter-pyridine bridge should also be included when ΔG^*_{in} is estimated for the $Co(bpy)_3^{2+}$–$Co(bpy)_3^{+}$ couple. This calculation cannot be done rigorously since knowledge of the force constant for this bond would require a complete vibrational analysis of the intra-bipyridine bonds in the complex, and this has not been done. However, a crude estimate of the reduced force constant f for C—C/C=C bonds of 6×10^5 dyn cm^{-1} may be obtained from literature values.[48] The latter, with $\Delta d_0 = 0.07$ (2) Å, gives a ΔG^*_{in} contribution of 3.3 kcal mol^{-1} after summing over the three bound bipyridines per complex. In light of the force constant problem and the uncertainty in Δd_0, $\Delta G^*_{in} = 3 \pm 1$ kcal mol^{-1} for the Co(II)–Co(I) couple seems a reasonable estimate at this time.

The parameters relevant to the $Co(bpy)_3^{3+}$–$Co(bpy)_3^{2+}$ and $Co(bpy)_3^{2+}$–$Co(bpy)_3^{+}$ exchange reactions are summarized in Table IX. The values of K_A, ΔG^*_{out}, and ΔG^*_{in} tabulated

(42) Phelps, D. W.; Kahn, E. M.; Hodgson, D. J. *Inorg. Chem.* **1973**, *14*, 2486.
(43) Ansell, C. W. G.; Lewis, J.; Liptrot, M. C.; Raithby, P. R.; Schroder, M. *J. Chem. Soc., Dalton Trans.* **1982**, 1593.
(44) Sutin, N. *Prog. Inorg. Chem.* **1983**, *30*, 441.
(45) Brunschwig, B. S.; Logan, J.; Newton, M. D.; Sutin, N. *J. Am. Chem. Soc.* **1980**, *102*, 5798.
(46) H. M. Neumann, quoted in: Farina, R.; Wilkins, R. G. *Inorg. Chem.* **1968**, *7*, 516.
(47) Krishnan, C. V.; Creutz, C.; Schwarz, H. A.; Sutin, N. *J. Am. Chem. Soc.*, in press.
(48) The C—C and C=C force constants used (4.5 and 9.5 mdyn $Å^{-1}$, respectively) in calculating the reduced force constant were taken from: Wilson, E. G., Jr.; Decius, J. C.; Cross, P. C. "Molecular Vibrations"; McGraw-Hill: New York, p 175, Table 8-1.

were discussed above. For the Co(II)–Co(I) exchange, parameters obtained by including intraligand changes are in square brackets. Note that the range in κ_n (calculated from eq 5) includes only the uncertainty in ΔG^*_{in} introduced by allowing an uncertainty of ±0.01 Å in the Δd_0 values. The ν_n values given were obtained from eq 7 by assuming a metal–ligand stretching vibration (410 cm^{-1}, 1.2×10^{13} s^{-1}) to be the dominant inner-shell mode for the Co(III)–Co(II) exchange and a C–C′ intraligand stretch (1400 cm^{-1}, 4.2×10^{13} s^{-1}) to be dominant for the Co(II)–Co(I) exchange (for both, $\nu_{out} = 0.9 \times 10^{12}$ s^{-1}). A small tunneling correction is implicated[3,45] for the Co(III)–Co(II) exchange and is included in the table; for the Co(II)–Co(I) couple Γ_n is negligible—1.3 with $\Delta G^*_{in} = 3$ kcal mol^{-1}. The last row in the column gives the value of the product $K_A \kappa_n \nu_n \Gamma_n = k/\kappa_{el}$. Comparison of the calculated products with the k_{obsd} values in the first row suggests that κ_{el} is not much less than 1; for both couples $\kappa_{el} \geq 0.2$, consistent with $\kappa_{el} \geq 10^{-2}$ recently implicated for a number of outer-sphere exchange reactions.[3] The calculated values for the Co(III)–Co(II) and Co(II)–Co(I) exchanges differ by about 7 orders of magnitude, in agreement with the measured rate ratio. This enormous reactivity difference has as its primary origin κ_n, with the difference between κ_n for the two couples being due entirely to ΔG^*_{in}. It is interesting that the agreement for the Co(III)–Co(II) couple is excellent if κ_{el} is taken equal to 1, but this should probably be viewed as coincidental since κ for this couple is so extremely sensitive to the value of Δd_0 taken (note that the 100-fold range in κ_n given for this couple in the table was obtained for the Δd_0 range of 0.18–0.20 Å). As noted above, the rate constant calculated for the $Co(bpy)_3^{2+}$–$Co(bpy)_3^{+}$ exchange does not change greatly when possible intraligand bonding changes are included. This reflects some cancellation in the ν_n and κ_n terms since increasing ΔG^*_{in} from 0.1 to 2 kcal mol^{-1} increases ν_n considerably (see eq 7).

The structural results for the tris(bipyridine)cobalt complexes taken with the semiclassical outer-sphere electron-transfer model thus provide a very satisfactory explanation of the extraordinary reactivity differences observed for the $Co(bpy)_3^{3+}$–$Co(bpy)_3^{2+}$ and the $Co(bpy)_3^{2+}$–$Co(bpy)_3^{+}$ couples. The reactivity difference is due to the fact that very large nuclear configuration changes accompany the reduction of $Co(bpy)_3^{3+}$ to $Co(bpy)_3^{2+}$ while those that accompany the reduction of $Co(bpy)_3^{2+}$ to $Co(bpy)_3^{+}$ are very small. These changes can, in turn, be related to the electronic configurations of the two couples. Unfortunately, decomposition of the Co(I) crystals precluded accurate characterization of the intra-bipyridine bonding in **2**. More accurate data would be desirable because the C–C and C–N bond lengths provide information about the extent of metal-to-ligand electron donation that would aid in clarifying the nature of the $Co(bpy)_3^{+}$ electronic structure. In addition, such information for $Co(bpy)_3^{+}$ and for low-oxidation-state species containing bpy^- would permit estimation of the contributions of intraligand bonding changes to the inner-shell electron-transfer barrier. Although we have made a preliminary attempt to include intraligand changes in this paper, detailed treatments for such couples as $Ru(bpy)_3^{3+}$–$^*Ru(bpy)_3^{2+}$ and $Ru(bpy)_3^{2+}$–$Ru(bpy)_3^{+}$ will require additional structural parameters and detailed vibrational analyses of the systems. It can be hoped that the semiclassical model that has served so well in explaining the role of metal–ligand bonding changes in determining electron-transfer rates[3] will be of equal value in accounting for the consequences of the intraligand bonding changes in such systems.

Acknowledgment. We wish to thank Drs. K. Barkigia, B. S. Brunschwig, R. Kirchner, and T. Koetzle for comments helpful to the progress of this work. This research was performed at Brookhaven National Laboratory under the auspices of the U.S. Department of Energy and supported by its Office of Basic Energy Sciences.

Registry No. **1**, 86119-86-0; **2**, 86119-87-1.

Supplementary Material Available: Table IV continued (Table S1), thermal parameters for the non-hydrogen atoms in **1** (Table S2), positional parameters for the hydrogen atoms in **1** (Table S3), observed and calculated structure factor amplitudes for **1** (Table S4), Table V continued (Table S5), thermal parameters for the non-hydrogen atoms in **2** (Table S6), positional parameters for the hydrogen atoms in **2** (Table S7), observed and calculated structure factor amplitudes for **2** (Table S8), a stereoview down *c* of the hydrogen bonding in $Co(bpy)_3Cl_2 \cdot 2H_2O \cdot EtOH$ (**1**) (Figure S1), a stereoview of the hydrogen bonding in **1** (Figure S2), a stereoview of the unit cell of $Co(bpy)_3Cl \cdot H_2O$ (**2**) (Figure S3), and a stereoview of the hydrogen bonding in **2** (Figure S4) (24 pages). Ordering information is given on any current masthead page.